J Mar Sci Technol (2006) 11:76–87
DOI 10.1007/s00773-006-0214-9

Journal of
Marine Science
and Technology

A study on improving the course-keeping ability of a pure car carrier in windy conditions

KAZUHIKO HASEGAWA[1], DONGHOON KANG[1], MASAAKI SANO[1], VISHWANATH NAGARAJAN[1], and MAKOTO YAMAGUCHI[2]

[1]Department of Naval Architecture and Ocean Engineering, Graduate School of Engineering, Osaka University, 2-1 Yamadaoka, Suita 565-0871, Japan
[2]Mitsui O.S.K. Lines, Ltd., Tokyo, Japan

Abstract The course-keeping ability of a pure car carrier (PCC) in windy conditions is discussed in this article. Numerical simulations of two PCCs were carried out to compare their course-keeping abilities in wind. The two PCCs had the same hull form but different types of rudder. One PCC was fitted with a semispade rudder (hereinafter, the normal rudder), whereas the other was fitted with a spade-type Schilling rudder (hereinafter, the Schilling rudder). Both PCCs were designed to a new concept for the accommodation structure and hull form above the load water line. In this new design concept, there are no sharp corners in the superstructure so as to reduce wind resistance and improve steering performance. The limits of course keeping for the two PCCs were investigated through simulations. The course-keeping abilities of the two PCCs, each with two different types of autopilot system, were also investigated in wind. To develop the numerical simulation, the hydrodynamic coefficients of the two PCCs were predicted based on the data published for a third PCC having similar principal particulars. The numerical model of the two PCCs was validated by comparing its behavior with the respective full-scale trial results. Wind resistance coefficients were predicted by combining the results of wind tunnel experiments of the object PCCs and a regression model. Numerical simulations under steady wind conditions were also carried out and the results compared with some full-scale experiments to validate the mathematical model of the PCC.

Key words PCC · Schilling rudder · Wind resistance · Course-keeping ability · Autopilot

List of symbols

A	effective projected area (*breadth* × *freeboard*)
A_R	rudder area
C_b	block coefficient
d	ship draft
d_e	perpendicular distance between the ship and the original route
D_P	propeller diameter
H_R	rudder height
I_{zz}	yaw moment of inertia
J'_{zz}	nondimensional added yaw moment of inertia
K_T	thrust coefficient
L	ship length
m	ship mass
$m'_x = m_x \Big/ \frac{1}{2}\rho L^2 d$	nondimensional added mass in surge
$m'_y = m_y \Big/ \frac{1}{2}\rho L^2 d$	nondimensional added mass in sway
n	propeller speed (rps)
N_{HP}, N_R, N_A	yaw moment components of hull–propeller, rudder, and wind acting on ship
N'_β, N'_r, $N'_{\beta\beta\beta}$, $N'_{\beta\beta r}$, $N'_{\beta rr}$, N'_{rrr}	nondimensional hydrodynamic coefficients of yaw moment
O	midship
P	propeller pitch
r	yaw rate at origin of ship-fixed coordinates
r_G	yaw rate at ship's center of gravity
t_P	thrust deduction factor
u_G	surge velocity at ship's center of gravity
U	ship velocity
U_A	relative wind velocity
v_G	sway velocity at ship's center of gravity
x_G	distance between ship's center of gravity and ship's center
X_H, X_P, X_R, X_A	x-axis components of hull, propeller, rudder, and wind force acting on ship
X'_0, $X'_{\beta\beta}$, $X'_{\beta r}$, X'_{rr}, $X'_{\beta\beta\beta\beta}$, $X'_{\beta\beta\beta r}$	nondimensional hydrodynamic coefficients of surge force
Y_{HP}, Y_R, Y_A	y-axis components of hull–propeller, rudder, and wind force acting on ship
Y'_β, Y'_r $Y'_{\beta\beta\beta}$, $Y'_{\beta\beta r}$, $Y'_{\beta rr}$, Y'_{rrr}	nondimensional hydrodynamic coefficients of sway force
β	drift angle
Λ	ruddar aspect ratio
ρ	water density

Address correspondence to: D. H. Kang
(Kang_Dong_Hoon@naoe.eng.osaka-u.ac.jp)
Received: July 25, 2005 / Accepted: January 5, 2006

ρ_A	air density
ω_{P0}	effective wake fraction coefficient for propeller inflow in straight running
ψ_A	relative angle of wind encounter
ψ_e	angle of deviation of heading angle from the original course

Introduction

With the increase in shipping trade, many ships are being constructed with large superstructures; particular examples are pure car carriers (PCCs) and liquefied natural gas (LNG) carriers. These ships are characterized by their high wind resistance compared to conventional ships because of their large superstructures. PCCs are especially severely affected by wind because of the low specific gravity of their cargo.

Wind often causes ship drift and changes in heading angle during a voyage. When a PCC deviates from its original course because of strong wind, its course-keeping ability is compromised. Additionally, if the PCC also lacks maneuverability, then it may become uncontrollable under severe wind conditions, even while using the rudder. Therefore, reducing the wind influence and increasing controllability for a PCC are very important for its performance in at sea.

Much effort has been spent on the reduction of wind influence and improving controllability of ships. Modifying the superstructure is one of the methods of reducing wind resistance. Smooth corners on the superstructure reduce the wind resistance compared to square corners. To improve controllability, special rudder systems such as the Schilling rudder system have been introduced.[1] It has already been proved that the Schilling rudder can provide a larger rudder force than a normal rudder.

In this paper, PCCs with improved superstructure design by Matsumoto[2] for reducing wind force were used. A Schilling rudder was fitted to one PCC to improve its maneuverability; the other PCC was fitted with a normal rudder. The efficiency of the two PCCs was compared using real-time maneuvering data and numerical simulations.

Recent vessels are fitted with improved navigational equipment such as global positioning systems (GPS) and autopilots. The accuracy of this equipment in generating maneuvering data has been well researched.[3] So in this article, data from full-scale experiments generated using this equipment were used to validate the numerical simulation models of the PCCs.

Table 1. Principal particulars of the model ship

L	3.000 m	$A_R/L{\cdot}d$	0.019
B	0.514 m	Λ	1.35
d	0.145 m	D_P	0.105
x_G	−0.087 m	D_P/H_R	0.992
C_b	0.539	P/D_P	1.042

Model ship

Two PCCs with the same hull forms but different types of rudder were used in this research for full-scale trials and numerical simulation. One ship was installed with a normal rudder, and the other was installed with a Schilling rudder. Both ships were scaled down to a model having an length between perpendiculas (LBP) of 3 m for the purpose of simulation; the scale ratio is 62.7. The main particulars of the model ship are shown in Table 1.

Equations of motion

The mathematical model for ship maneuvering is described based on the three degrees of freedom surge, sway, and yaw. The equations for ship maneuvering are written as:

$$\begin{aligned} m\dot{u}_G - mv_G r_G &= X \\ m\dot{v}_G + mu_G r_G &= Y \\ I_{ZZ}\dot{r}_G &= N - x_G Y \end{aligned} \tag{1}$$

The external forces X, Y, and moment N consist of hull, hull and propeller, and rudder and wind components as follows:

$$\begin{aligned} X &= X_H + X_P + X_R + X_A \\ Y &= Y_{HP} + Y_R + Y_A \\ N &= N_{HP} + N_R + N_A \end{aligned} \tag{2}$$

Figure 1 shows the coordinate system and definition of various parameters.

Hull forces and moment

Hydrodynamic hull coefficients are usually determined from model tests, but the model test for the PCC studied in this paper was not carried out. Yoshimura[4] has published hydrodynamic coefficients of a PCC (hereinafter, Yoshimura's PCC) based on model tests. The principal particulars of Yoshimura's PCC are similar to the PCCs studied in this article, so the hydrodynamic coefficients of the PCC studied here are predicted by modifying those of Yoshimura's PCC. The prediction of

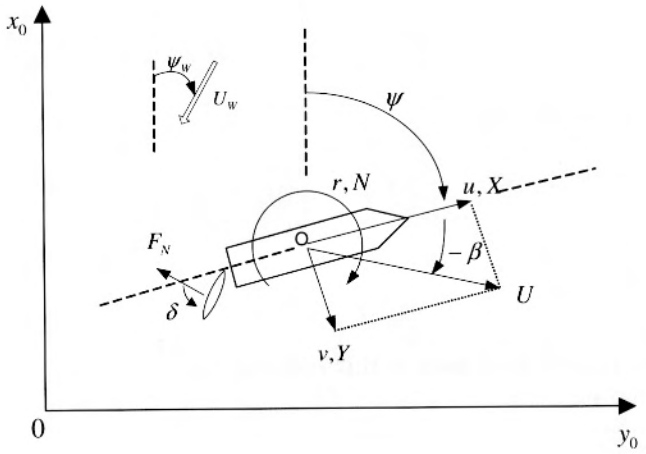

Fig. 1. Coordinate systems

Table 2. Coefficients of thrust model

a_1	0.566	t_P	0.165
a_2	−0.4593	ω_{P0}	0.222
a_3	−0.0286		

hydrodynamic coefficients is discussed in the next section. For estimating the hull forces and moment, the following equations were used:

$$\begin{aligned} X'_H &= -m'_x\dot{u}'_G + X'_0 + X'_{\beta\beta}\beta^2 + \left(X'_{\beta r} - m'_y\right)\beta r' + X'_{rr}r'^2 \\ &\quad + X'_{\beta\beta\beta\beta}\beta^4 + X'_{\beta\beta\beta r}\beta^3 r' \\ Y'_{HP} &= -m'_y\dot{v}'_G + Y'_\beta\beta + \left(Y'_r - m'_x\right)r' + Y'_{\beta\beta\beta}\beta^3 + Y'_{\beta\beta r}\beta^2 r' \\ &\quad + Y'_{\beta rr}\beta r'^2 + Y'_{rrr}r'^3 \\ N'_{HP} &= -J'_{ZZ}\dot{r}'_G + N'_\beta\beta + N'_r r' + N'_{\beta\beta\beta}\beta^3 + N'_{\beta\beta r}\beta^2 r' \\ &\quad + N'_{\beta rr}\beta r'^2 + N'_{rrr}r'^3 \end{aligned} \tag{3}$$

Propeller force

The mathematical model for the thrust produced by the propeller is made up of Eqs. 4 and 5. Coefficients of propeller thrust for the PCC from experimental data are given in Table 2.

$$X'_P = 2\left(1-t_P\right)K_T\left(D_P^2/Ld\right)/J_S^2 \tag{4}$$

$$\left.\begin{aligned} K_T &= a_1 + a_2 J + a_3 J^2 \\ J &= \left(1-\omega_{P0}\right)u/nD_P \\ J_S &= U/nD_P \end{aligned}\right\} \tag{5}$$

Rudder forces and moment

In this article, a normal rudder and a Schilling rudder were used for the simulation. A perspective view and

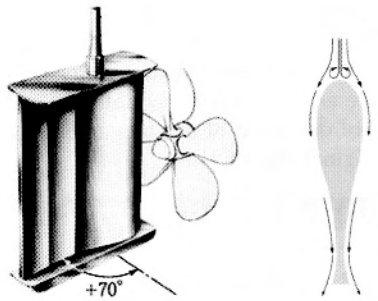

Fig. 2. Perspective view and section of Schilling rudder

section of the Schilling rudder are shown in Fig. 2. The unique profile of the Schilling rudder incorporates a rounded leading edge and a fishtail trailing edge. The Schilling rudder is well known for utilizing the propeller slipstream to achieve an efficient "side thrust" effect at the ship's stern with operating angles of up to 70°. However, in this research the maximum angle of the Schilling rudder was restricted to 35° for easy comparison with the normal rudder. When the dimensions of the Schilling rudder and the normal rudder are the same, the normal force coefficient for the Schilling rudder can be expressed from that of the normal rudder by multiplying it by some constant factor.[5]

In this article, the normal force coefficient for the Schilling rudder is 1.3 times the normal force coefficient of the normal rudder. Also, the normal rudder and the Schilling rudder in the full-scale trials and simulation had the same size and aspect ratio.

The coefficients for the mathematical model of the normal rudder were estimated from Yoshimura's rudder model. This is because the hull form and rudder aspect ratio of the PCC fitted with the normal rudder are similar to that of Yoshimura's PCC.

Wind forces and moment

Only the forces induced by a steady wind were considered in this article. The expressions of the forces and moment induced by the wind are as follow:

$$\left.\begin{aligned} X_A &= \frac{1}{2}\rho_A A U_A^2 C_{FX}\left(\psi_A\right) \\ Y_A &= \frac{1}{2}\rho_A A U_A^2 C_{FY}\left(\psi_A\right) \\ N_A &= \frac{1}{2}\rho_A A U_A^2 L C_{MZ}\left(\psi_A\right) \end{aligned}\right\} \tag{6}$$

where C_{FX}, C_{FY}, and C_{MZ} are wind force coefficients.

For an encounter angle of 0°–60°, the wind forces acting on the PCC were obtained from wind tunnel experiments carried out by Matsumoto.[2] Fujiwara's formula[6] was used to estimate the wind forces and moment

Table 3. Parameters of Fujiwara's formula

A_T	0.261 m²	C_{BR}	−0.048 m
A_L	1.492 m²	H_{BR}	0.363 m
A_{OD}	0.069 m²	H_C	0.156 m
C	−0.03 m		

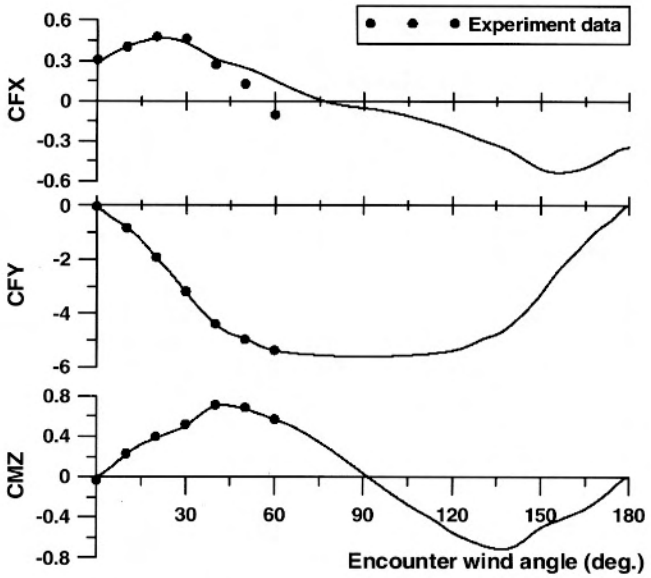

Fig. 3. Coefficients of wind resistance. *CFX*, *CFY*, force coefficients in *x*- and *y*-direction; *CM2*, coefficient of moment in *z*-direction

for encounter angles of 60° to 180°. The parameters used for estimating wind forces are shown in Table 3. The wind forces and moment obtained from Fujiwara's formula were modified based on the results from the wind tunnel experiment to obtain a smooth and continuous extension of the curve from the experiment. The wind resistance coefficients C_{FX},C_{FY}, and C_{MZ}, which are used in the numerical simulations, are shown in Fig. 3 as functions of the wind encounter angle.

Autopilot

Two types of proportional–differential (PD) controllers were adopted for course keeping of the model ship. The two control equations are:

$$\text{type 1} \quad \delta_{order} = C_1\psi_e + C_2 r$$
$$\text{type 2} \quad \delta_{order} = C_1\psi_e + C_2 r + C_3 d_e \qquad (7)$$

Type 1 autopilots control the rudder angle referring to the heading angle and yaw rate, whereas Type 2 additionally include the path error (d_e). The coefficients were set as $C_1 = 3.5$, $C_2 = -0.9$, and $C_3 = 50$ by repeated simulation of course keeping under a particular wind condition. The coefficients were calculated only for the normal rudder. For ease of comparison, the same values of the coefficients were used for the Schilling rudder.

Estimation of hull forces and moment

As mentioned earlier, the hydrodynamic coefficients of the PCCs studied in this paper were not available; for the simulation, it is necessary to estimate hydrodynamic coefficients. Initially, simulation was done using the hydrodynamic coefficients for Yoshimura's PCC. Predictably, the results of the simulation did not match those from the full-scale trial. The hull form of Yoshimura's PCC is not exactly the same as that of the PCCs studied in this paper, so the hydrodynamic coefficients needed modifying. To modify the hydrodynamic coefficients, the sensitivities of the coefficients were examined by carrying out simulations. The hydrodynamic coefficients that affect the ship's velocities were identified by sensitivity analysis,[7] and then tuned by repeated simulation and simultaneous comparison with full-scale trials. It may be noted that three sets of hydrodynamic coefficients, including in shallow water conditions, were available for Yoshimura's PCC. The effect of the shallow water significantly affects ship's motion and cannot be neglected in shallow water condition[8,9]. However, the full-scale trials in this paper were carried out at water depths which are more than 10 times of ship's draft. Because of above reason, the effect of shallow water was not considered and the hydrodynamic coefficients of Yoshimura's PCC for deep water condition were used in this paper.

Sensitivity analysis

Initially, simulations with the original set of hydrodynamic coefficients obtained from Yoshimura's PCC were carried out. The simulations were then repeated, increasing each hydrodynamic coefficient by 20%. Both sets of simulations were then compared. An index of sensitivity S was defined as the sum of the squares of the differences in velocities between the two sets of simulations.

$$S = \left(\sum_{t=0}^{t} \left(v_o(t) - v_s(t) \right)^2 + \sum_{t=0}^{t} \left(r_o(t) - r_s(t) \right)^2 \right) \times 100 \qquad (8)$$

where S is the sensitivity of hydrodynamic coefficients, v_o and r_o are the values obtained during simulation with the hydrodynamic coefficients of Yoshimura's PCC, and v_s and r_s are the values obtained during simulation with each of above hydrodynamic coefficients increased in turn by 20%.

The sensitivities of only those hydrodynamic coefficients used in the sway and yaw equations were com-

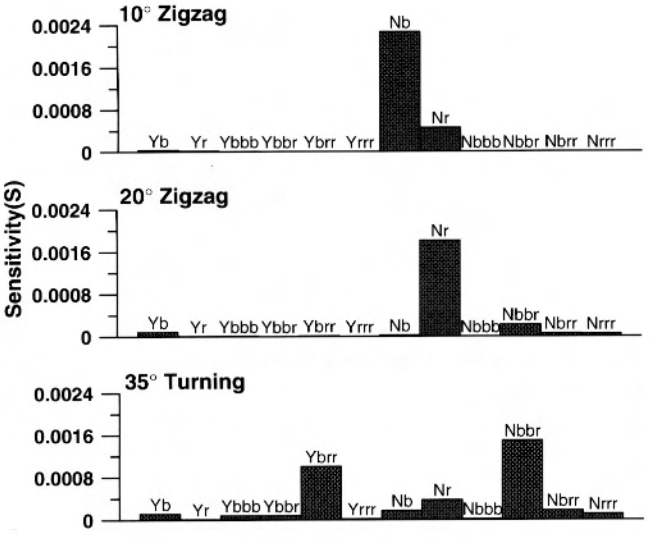

Fig. 4. Sensitivities of hydrodynamic derivatives

puted. Also, only the above-mentioned hydrodynamic coefficients were modified. This is because the turning ability and course-keeping ability are the focus of this sensitivity analysis; therefore, only v and r are considered in Eq. 8.

The sensitivity analysis was carried out for 10° and 20° zigzag tests and a 35° turning test. The hydrodynamic coefficients significantly affecting each of the above tests were thus identified. Figure 4 shows the results of the sensitivity examination.

Comparison with full-scale trials

Simulation of 10° and 20° zigzag tests and a 35° turning test was carried out by varying only the sensitive hydrodynamic coefficients related to each test. The results from the simulation and the full-scale trials were compared. A trial-and-error method was used to predict the hydrodynamic coefficients for the PCCs. Initially, changes in the hydrodynamic coefficients for the 10° zigzag test were considered. This is because the 10° zigzag test has the least number of hydrodynamic coefficients that significantly affect the ship's sway and yaw motion as shown in Fig. 4. The hydrodynamic coefficients that affect the 10° zigzag test were tuned until the simulation results matched those of the full-scale trial results. The same procedure was then performed for the 20° zigzag test and finally for the 35° turning test. It should be noted that the targeted comparison between the simulation and the full-scale trials was the main focus while tuning. After obtaining one set of hydrodynamic coefficients, the simulation and tuning process was again started from the 10° zigzag test. The entire procedure was repeated until simulation of all three tests matched the results of the full-scale trials.

Table 4. Variation of hydrodynamic derivatives from Yoshimura's PCC

$Y'_{\beta r}$	−25%	N'_r	30%
N'_β	−30%	$N'_{\beta\beta r}$	25%

PCC, pure car carrier

The maximum allowable variation in the hydrodynamic coefficients was set at 30% of the original value. This is because the hull form of the PCCs studied in this paper is similar to that of Yoshimura's PCC. The variation of the hydrodynamic coefficients from those of Yoshimura's PCC is shown in Table 4.

The accuracy of the simulation with the tuned hydrodynamic coefficients was validated by comparing the results obtained with the results from full-scale trials. Comparisons of the full-scale trial results and the simulations for a PCC with a normal rudder are shown in Fig. 5. It is noted that while the simulations of 10° and 20° zigzag tests are in good agreement with full-scale trials, there are some discrepancies between the results from the simulation and the full-scale trials in the case of the ±35° turning tests. During the full-scale Turning tests, the wind conditions were not measured, so the wind force could not be included in the simulation. Therefore, the difference may possibly be attributable to the influence of wind forces.

The above-mentioned simulations and calculations were also done for a PCC fitted with a Schilling rudder. Figure 6 shows the comparisons between the simulations and the full-scale trials with the Schilling rudder. In this case also, the results from the simulations agree with those from the full-scale trials except for the case of the +35° turning test. Here also, the difference in results can be attributed to the wind forces, as explained for the case of the normal rudder. The wind conditions were not measured for the turning tests, so it is difficult to tell if any particular test was influenced by wind. The modified coefficients may not have optimum values for the subject PCCs for the above reasons. However, the established simulation model with the modified coefficients was considered to be suitable for use in the next stage of analysis. To reduce the uncertainty in the simulation model, the model was validated again in windy conditions.

Validation of simulation in wind

The mathematical model developed in the previous section was validated for the PCC with the Schilling rudder by conducting a full-scale trial. Validation was carried out only for the PCC fitted with the Schilling rudder

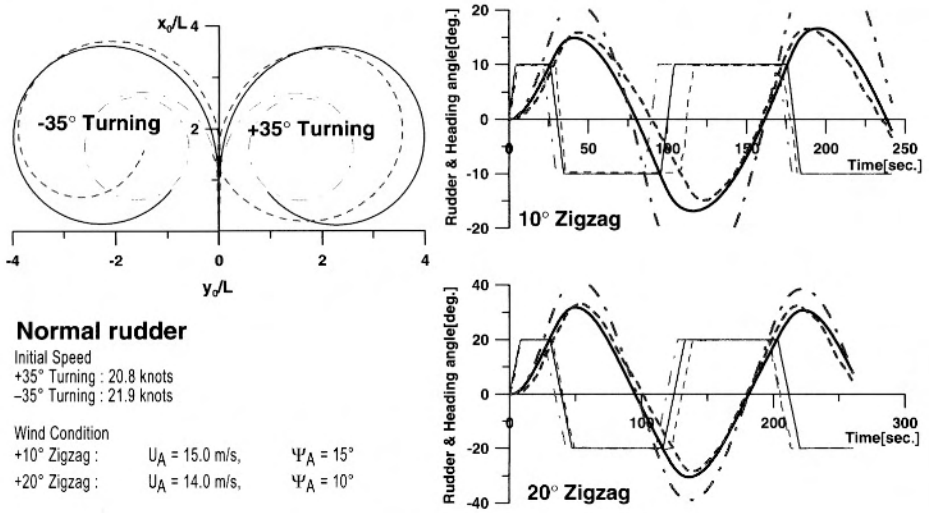

Fig. 5. Comparison between full-scale trials (*dashed lines*) and simulations with normal rudder. *chained lines*, simulation using Yoshimura's coefficients; *solid lines*, simulation using tuned coefficients

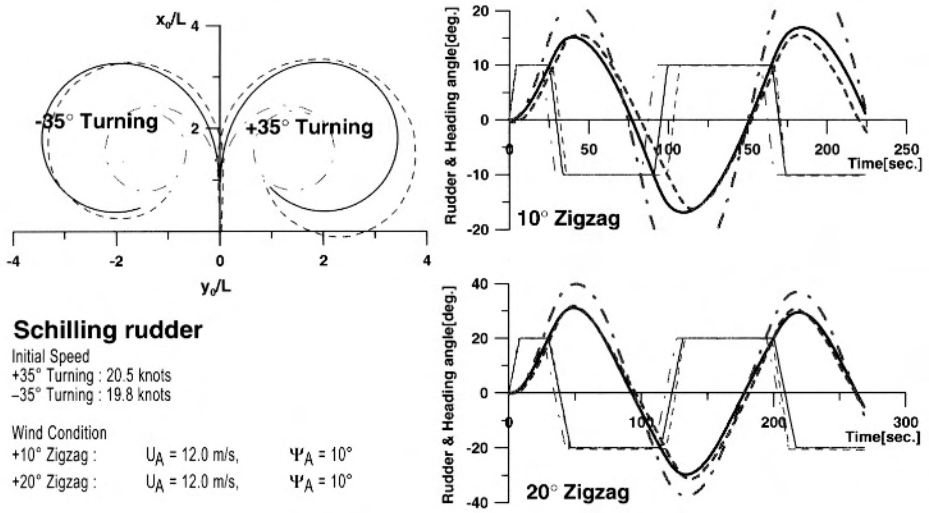

Fig. 6. Comparison between full-scale trials and simulations with Schilling rudder

because only this ship was equipped with the necessary measurement instruments. The drift angle of the PCC was calculated from gyroscope and GPS data. Readings from the gyroscope and autopilot were taken at 0.8-s intervals; readings from the GPS were taken at 1-min intervals. The conditions of the wind and waves were noted during the trials by the onboard helmsman. This is because recording functions were not available on the wind and wave measuring instruments. These conditions were noted according to the instruments indicators. In total 11 runs were recorded; the conditions of the trials are shown in Table 5. The numbering of the trials has been done on the basis of the relative wind direction. Runs 1, 4, 5, 8, 9, and 11 were for course keeping and course alteration; the remaining cases were for course keeping only. To validate the mathematical model of the PCC with the Schilling rudder, the simulations were carried out for the same wind conditions that were prevailing during the trials. The wind speed and direction are assumed to be constant, and the effect of the waves is ignored in the simulation. The type 1 autopilot was used for these simulations and for the full-scale trials.

Figure 7 shows an example of the course-keeping simulation corresponding to run 10 of the full-scale trials. The trajectory of the simulation compares favorably with that of the full-scale trial. Because the simulation was carried out assuming steady wind conditions, even though the conditions varied a lot during the full-scale experiment (which was carried out for quite a long duration), the time histories of the rudder angle and the drift angle cannot be compared. Therefore, the mean rudder angle and the mean drift angle were used for comparison as, shown in Fig. 7. The mean rudder

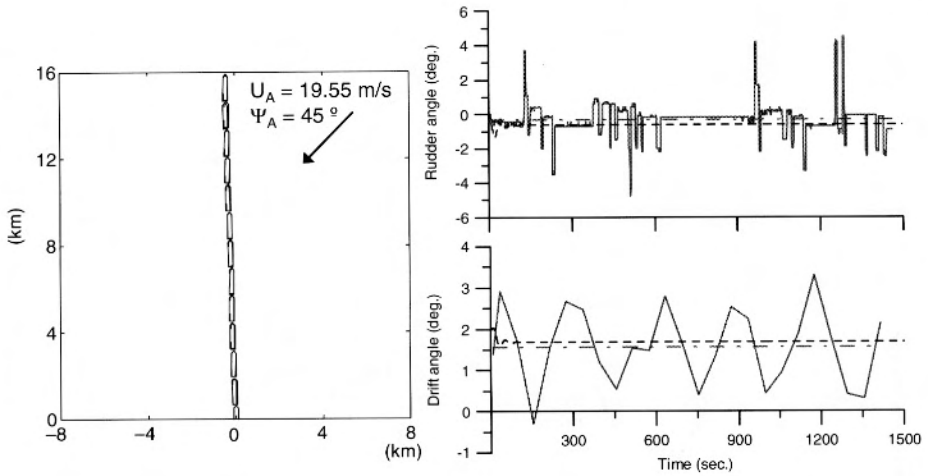

Fig. 7. Example of coursekeeping simulation. *solid lines*, full-scale trial; *chained lines*, average of the trial; *dashed lines*, simulation

Table 5. Conditions of full-scale experiments

No.	Relative wind angle (deg.)	Relative wind speed (m/s)	Relative wave angle (deg.)	Wave height (m)
1	0	7.72	0	0.5
2	−7	10.29	−10	0.5
3	10	9.26	10	1
4	10	10.29	10	0.5
5	25	19.03	25	2
6	−30	18.52	−30	3
7	−30	19.03	−30	2
8	35	10.8	35	1
9	35	23.15	35	3
10	45	19.55	45	2
11	−50	21.09	−50	2

Deg., degrees

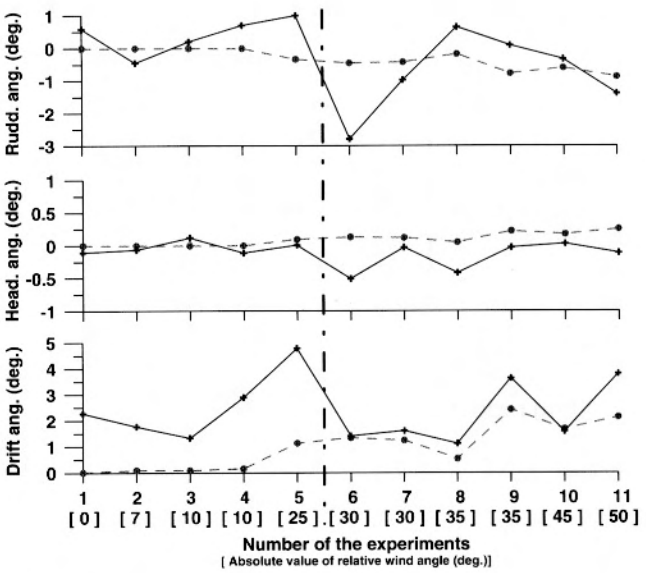

Fig. 8. Comparison of rudder angle and drift angle between simulations (*dashed lines*) and experiments (*solid lines*)

angles, the mean heading angles, and the mean drift angles of the simulations and the trials are summarized in Fig. 8. It should be noted that on the graphs for each run, the relative wind angle is shown as a positive value, so for the runs where the actual relative wind angle was negative, the rudder angle, the heading angle, and the drift angle must be interpreted as having the opposite sign to that shown on the graph.

For the mean drift angle in the range of 30°–50° of relative wind direction, there is good agreement between the simulations and the trials. Assuming that the mean drift angle represents the drift angle for steady yaw motion, it can be considered that the modified hydrodynamic coefficients have been properly estimated for the target PCC. This is because the drift angle has been shown to be a function of only nondimensional sway and yaw hydrodynamic forces and the nondimensional wind force.[10] However, some differences appear in the range of 0°–25° relative wind direction. This is because in the range 30°–50°, the wind force has greater significance than the other forces, whereas in the range 0°–25°, external forces other than wind are significant. It is noted that there are differences in the mean rudder angle between the simulations and full-scale trials. For the rudder angle, this difference is also caused by the factors mentioned above. For the heading angle, it is difficult to judge whether the simulations match the experiments because both results have a very small heading angle.

The course alteration experiments were carried out for ±20° course alterations, using ±10° of rudder. Figure 9 shows the course alteration simulation corresponding to run no. 4 of the full-scale trial and illustrates that the mathematical model accurately simulates rudder angle and heading angle. It is noted that after about 70 s, small rudder angles appear during the trial. This is because the autopilot was started at that time after the course

Table 6. Comparison of rudder operation time for +20° course alteration

No.	Experiment A (s)	Simulation A (s)	Experiment B (s)	Simulation B (s)
1	33.6	26.7	6.4	9.7
4	34.4	26.7	4.8	9.7
5	34.4	23.5	9.6	9.4
8	30.4	28.3	5.6	9.8
9	28.8	25.9	0.8	9.8
11	33.6	29.9	7.2	7.5
Average	32.5	26.8	5.7	9.3

A, time to initiate the turn; B, time to stop the turn

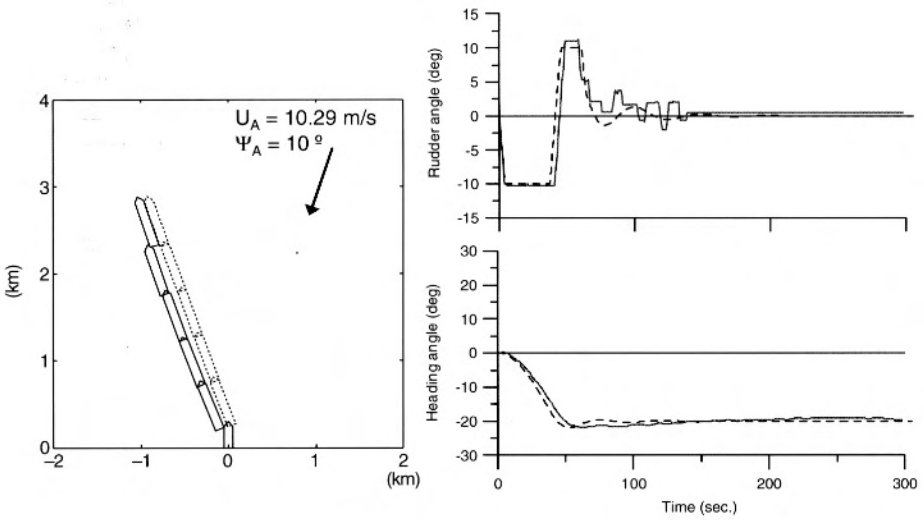

Fig. 9. Example of course alteration. *solid lines*, full-scale trial; *dashed lines*, simulation

alteration. The duration of the rudder angle required for course alteration during the simulation and the full-scale trial were also compared. The duration of the rudder angle, A and B, given during the course alteration is defined in Fig. 10. The rudder is put over to a given angle for time A to initiate the turn, and then an identical counter rudder angle is applied for time B to stop the turn. Table 6 shows the times A and B for the simulation and the trial during a +20° course alteration. Similarly, Table 7 shows the comparison for a course alteration of –20°. Times A for experiments and simulations are comparable, although some simulation results for the +20° course alteration show more than 20% variation. Overall, the results of simulations relate well to the experimental results. However, for time B, run nos. 4, 9 (for +20°), and 9 (for –20°) the simulated values and the trials do not agree. It may be noted that in the above three cases of course alteration in the trials, the autopilot was started prior to completion of the course alteration, so time B is calculated approximately, which may have resulted in the deviations mentioned above.

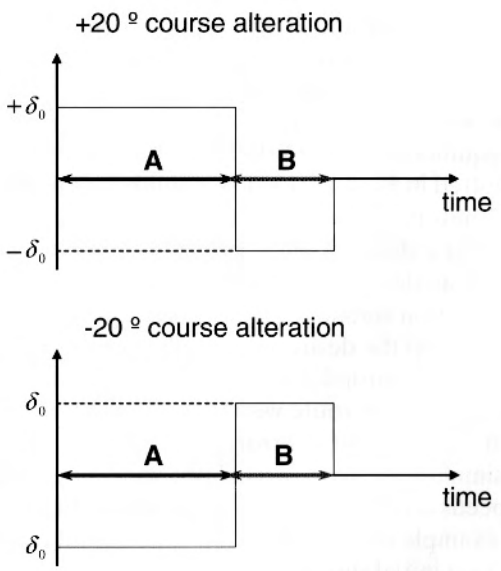

Fig. 10. Definition of rudder operation times

Table 7. Comparison of rudder operation time for –20° course alteration

No.	Experiment A (s)	Simulation A (s)	Experiment B (s)	Simulation B (s)
1	36.0	33.0	10.4	9.4
4	36.8	33.0	9.6	9.7
5	34.4	32.3	6.4	8.9
8	37.6	28.3	6.4	9.3
9	32.8	29.9	3.2	9.0
Average	35.5	31.3	7.2	9.3

From the above comparisons, it can be concluded that the mathematical model of the hull and wind forces can accurately simulate the maneuvering motion of the PCC, although there may be some minor discrepancies between the simulations and the experiments. No validation of the mathematical model was carried out for the PCC with the normal rudder because the PCCs are the same in all respects except for the rudder.

Limit of course-keeping ability

In this section, the course-keeping abilities of the PCC with a normal rudder and the PCC with a Schilling rudder are compared by carrying out simulations. The course-keeping abilities are investigated using both the type 1 autopilot and type 2 autopilot. The maximum rudder rate for both types of rudder was set at 19.0°/s for the model scale (this corresponds to 2.4°/s for the full-scale ship). The simulations were carried out from 0° to 180° of wind encounter angle. The initial speed of the ship was set to 5, 10, and 20 knots corresponding to the full-scale ship. The ratio of wind velocity and ship's initial velocity (hereinafter, the wind rate) was set at 2, 4, and 6. The values of the drift angle and the rudder angle at the equilibrium point relative to the wind conditions are plotted in Figs. 11–13. The equilibrium point for the type 1 autopilot is defined as the state at which the ship keeps the desired heading angle with certain rudder and drift angles. The type 2 autopilot is designed for positional motion stability. The distance gain (d_e) in Eq. 7 is used to keep the desired track. The equilibrium point for the type 2 autopilot is defined as the state at which the ship keeps her route with some error margin, i.e., with both ψ_e error and d_e error.

First, the simulations were carried out with different initial ship speeds and the same wind conditions. Figure 11 shows an example of the simulation with a wind rate of 4 and different initial ship speeds. The drift angles are the same for the same wind conditions even when using different rudders. The angles of the Schilling rudder are smaller than those of the normal rudder. In these simulations, it was observed that the rudder angle and the

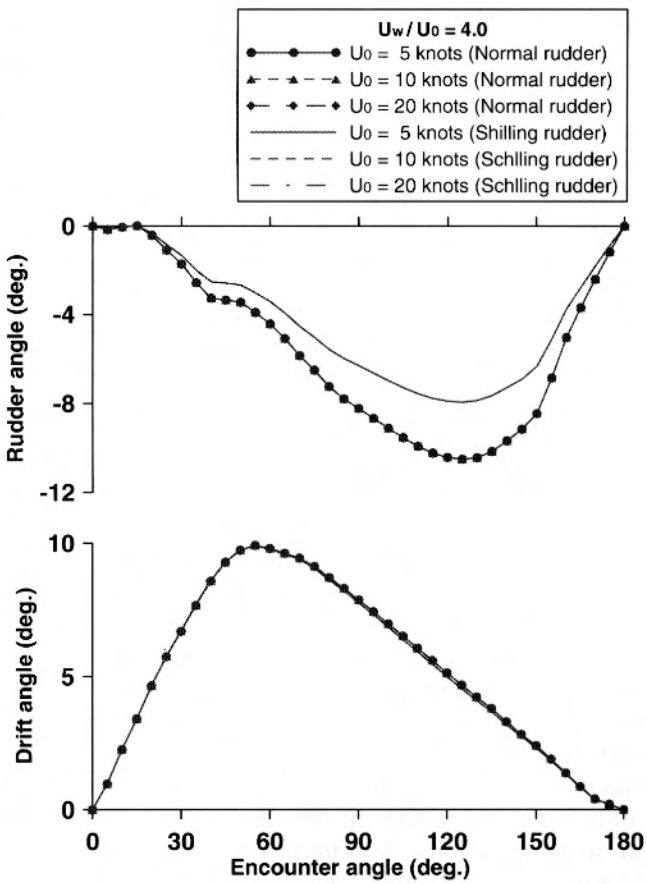

Fig. 11. Rudder and drift angle of the simulation for course keeping with the type 1 autopilot and various ship speeds

drift angle were not governed by the initial speed. Figure 12 shows the drift angle and rudder angle calculated using different wind conditions for the normal rudder and the Schilling rudder. For low wind speeds, both types of rudder show the same drift angle; however, the angles for the Schilling rudder are smaller than those for the normal rudder. At an encounter angle of about 140° for a wind rate of 6, the PCC with the normal rudder can not keep its course, even with the maximum rudder angle. This state is marked as "out-of-control." However, for the same wind rate, the PCC with the Schilling

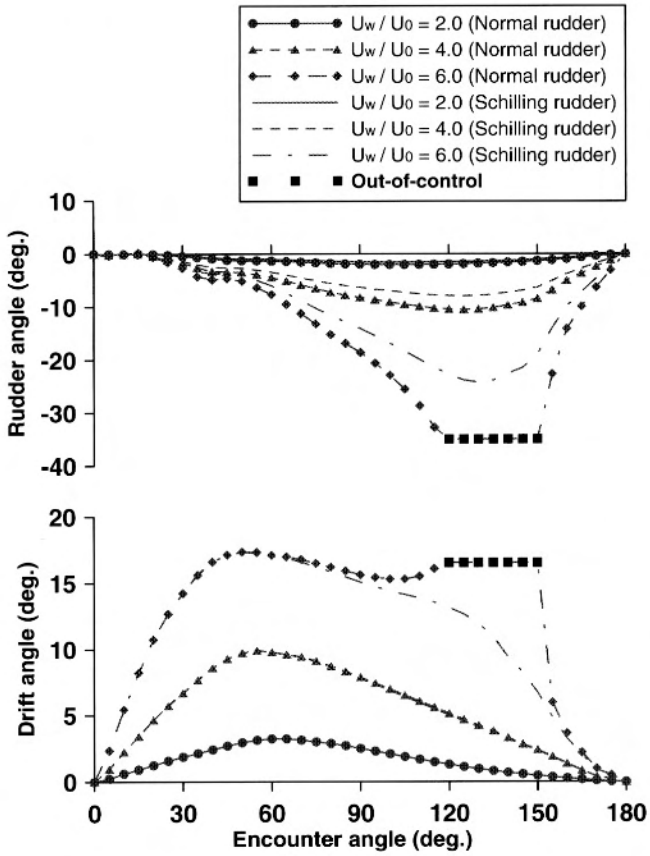

Fig. 12. Rudder and drift angle of the simulation for course keeping with the type 1 autopilot and various wind speeds

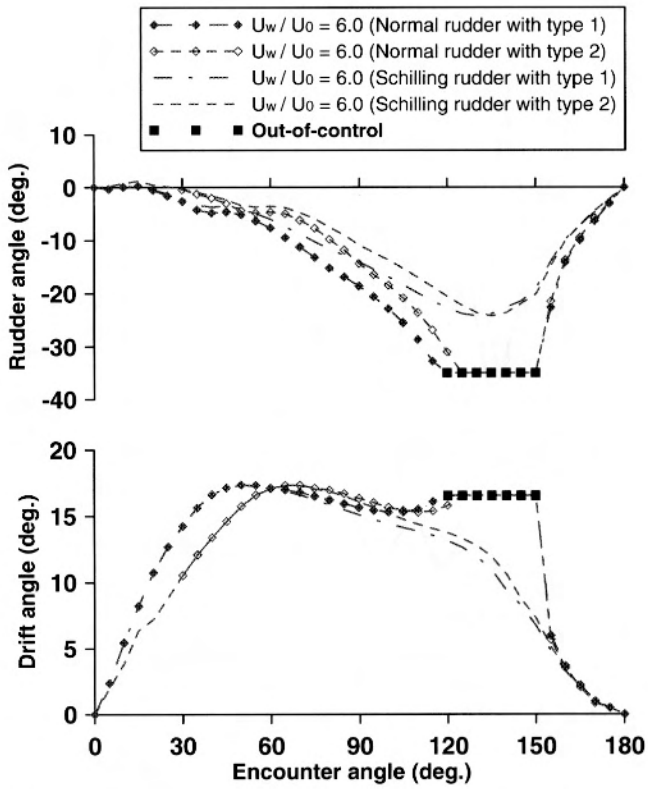

Fig. 13. Rudder and drift angle of the simulation for course keeping and track keeping with type 1 and type 2 autopilots

rudder was able to keep its course. The results clearly show that the PCC with the Schilling rudder has more course-keeping ability than the PCC with the normal rudder.

Figure 13 shows the rudder angles and drift angles for type 1 and type 2 autopilots for various encounter angles for a wind rate of 6. An equilibrium point does not appear from 5°–25° of wind encounter angle for a normal rudder with type 2 autopilot. Figure 14 shows the trajectories of the simulations for the four cases corresponding to a 25° wind encounter angle and a wind rate of 6. The results of simulations with the type 1 autopilot were not much different for the normal rudder and the Schilling rudder. In both cases, the ships keep their desired courses even though they were deviated from their route by wind. The results of simulations with the type 2 autopilot are quite distinct between the normal rudder and the Schilling rudder. The Schilling rudder has sufficient controllability to keep the course and route. However, for the normal rudder the ship's movement becomes uncontrollable. It should be noted that the autopilot coefficients directly influence the performance of the autopilot, so the simulation was carried

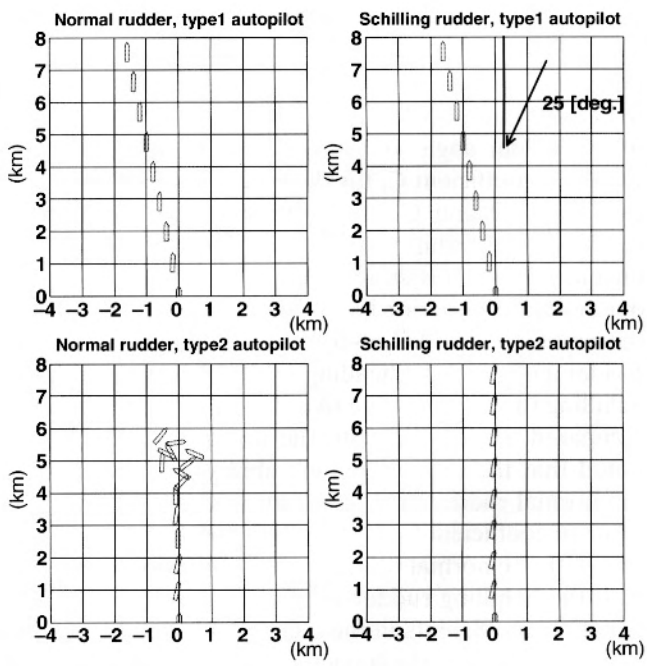

Fig. 14. Trajectories of the simulations at 25° wind encounter angle and a wind rate of 6

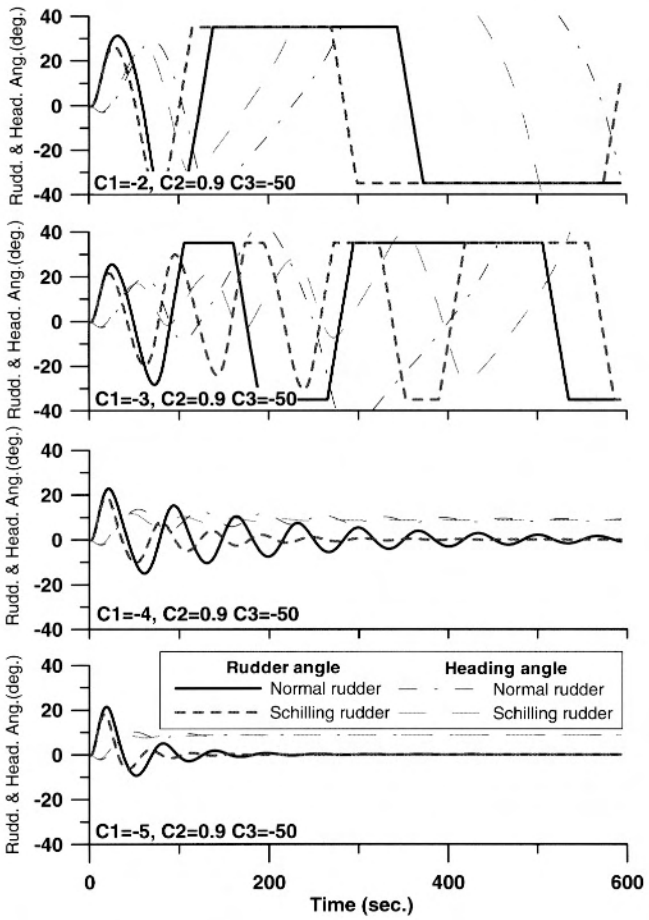

Fig. 15. Time histories of rudder angle with various values of coefficient C_1 for the type 2 autopilot at 25° wind encounter angle and a wind rate of 6

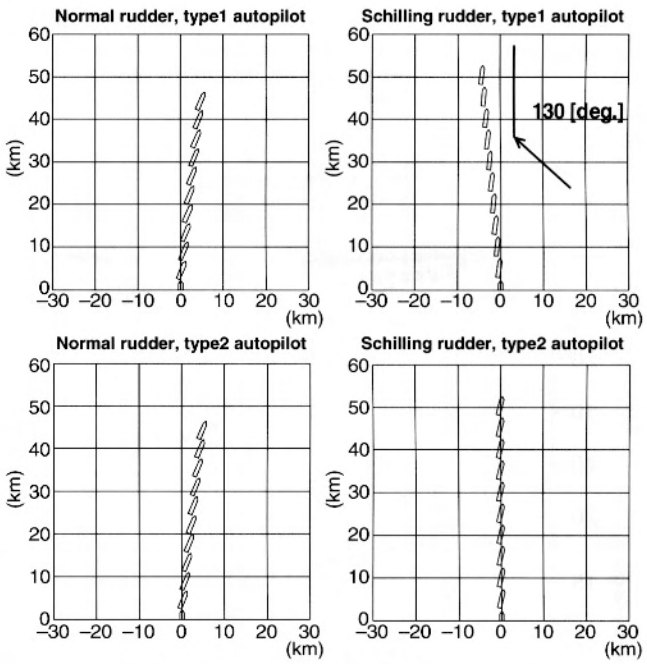

Fig. 16. Trajectories of the simulations at 130° wind encounter angle and a wind rate of 6

out again but with a different value for coefficient C_1 in the type 2 autopilot. Figure 15 shows the time histories of the rudder angle and the heading angle for various values of coefficient C_1 for the type 2 autopilot. For the case $C_1 = -2$ and $C_1 = -3$, the ship with the normal rudder and the ship with the Schilling rudder became uncontrollable. It is difficult to conclude that either rudder system is superior based on the above results. For the case $C_1 = -4$ and $C_1 = -5$, it is easily observed that the rudder angle and the heading angle of the ship with the Schilling rudder converge to a steady value much faster compared to the ship with the normal rudder. It was noted that the course-keeping ability of the ship with the normal rudder could be improved by changing the value of coefficient C_1; however, the performance of the ship with the normal rudder remains inferior to the ship with the Schilling rudder for the same set of autopilot equation coefficients in the controllable condition.

Figure 16 shows the trajectories of the simulations for a 130° wind encounter angle and a wind rate of 6. In this case the simulation had to be carried out much longer (100 min) compared with the simulation for the 25° wind encounter angle. It is cleaer that the vessel with the Schilling rudder with the type 2 autopilot has good position motion stability for this wind condition. In the case of the type 1 autopilot, the PCC with the Schilling rudder has directional stability even though the ship is drifted by the wind. The normal rudder with both types of autopilot used the maximum rudder angle; however, both ships gradually deviate from their course and routes. It is difficult to come to any conclusions about the relative performance of the Schilling rudder and the normal rudder with the type 1 autopilot by observing Fig. 16 alone. Therefore, the time histories of the longitudinal distance traversed by the ship and the heading angles for the normal rudder and the Schilling rudder with the type 1 autopilot are compared in Fig. 17. The ship with the Schilling rudder covers more distance compared with the ship with the normal rudder. This is because the ship with the normal rudder experiences more deviation from the base heading angle, and therefore the hull drag is greater compared to that of the PCC with the Schilling rudder. Additionally, for the normal rudder, the deviation of the propeller thrust from the ship's intended direction of motion is greater compared with the PCC with the Schilling rudder. In Fig. 17 it is seen that for the normal rudder, the ship's heading stabilizes after some time. This is because at this heading, the wind encounter angle substantially changes and the ship comes out of the out-of-control

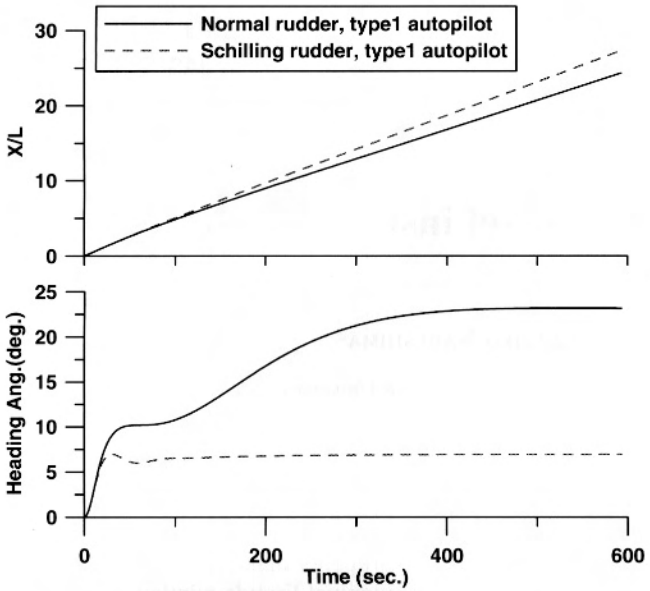

Fig. 17. Longitudinal distance and heading angle of the simulations at 130° wind encounter angle and a wind rate of 6

region of the normal rudder, but the ship still needs maximum rudder angle to proceed ahead.

Conclusions

In this article, improving the course keeping of a PCC in windy conditions is discussed. A Schilling rudder was shown to be one of the ways to improve the course keeping in wind. Simulation of a PCC with a Schilling rudder was carried out. Comparisons between the course-keeping and track-keeping ability of the vessels fitted with a normal rudder and a Schilling rudder were made. The outline of the article is as follows:

1. The hydrodynamic coefficients of the subject PCC were predicted by modifying the coefficients available for a similar PCC and by comparisons with full-scale trials. The maneuvering motion of the PCC was simulated successfully with the hydrodynamic coefficients calculated above.
2. Two different types of autopilot were investigated, both with a normal rudder and a Schilling rudder. Generally, the angle of the Schilling rudder was smaller than that of the normal rudder for the same wind conditions, even though the drift angle was the same.
3. With both types of autopilot, the normal rudder, even at its maximum rudder angle, could not keep the ship's course in certain wind conditions, but the Schilling rudder had sufficient controllability for the same wind conditions.
4. The Schilling rudder creates more lifting force than the normal rudder, therefore, the Schilling rudder is able to control the ship's movement in severe wind, even though it has the same maximum rudder rate as that of the normal rudder.

References

1. Kose K, Hosokawa M, Yamada H, et al (1992) A study on performance estimation of special rudders (in Japanese). Trans West Jpn Soc Nav Archit 84:49–57
2. Matsumoto K, Tanaka Y, Hirota K, et al (2003) Reduction of wind force acting on ships (in Japanese). J Kansai Soc Nav Archit 240:115–121
3. Ueno M (2000) A GPS-based system for precise shipping guidance and control. J Mar Sci Technol 5:9–15
4. Yoshimura Y (1986) Mathematical model for the maneuvering ship motion in shallow water (in Japanese). J Kansai Soc Nav Archit 200:41–51
5. DNV (1985) Hull equipment and appendages: stern frames, rudders and steering gears. Rules for classification of steel ships part3. Det norskeVeritas, Norway, Chap 3, Sect 2:2–19
6. Fujiwara T, Ueno M, Nimura T (1998) Estimation of wind forces and moments acting on ships (in Japanese). J Soc Nav Archit Jpn 183:77–90
7. Rhee KP, Kim KH (1999) A new sea trial method for estimating hydrodynamic derivates. J Ship Ocean Technol 3(3):25–44
8. Saha GK, Suzuki K, Kai H (2004) Hydrodynamic optimization of ship hull forms in shallow water. J Mar Sci Technol 9:51–62
9. McGookin EW, Murray-Smith DJ, Li Y, et al (2000) Ship steering control system optimisation using genetic algorithms. Control Eng Pract 8:429–443
10. Yasukawa H, Kose K (2004) Application of a simulation method for ship maneuverability to the maneuvering booklet (in Japanese). Trans West Jpn Soc Nav Archit 107:87–89